TENTH AUSTRALASIAN FLUID MECHANICS
CONFERENCE - UNIVERSITY OF MELBOURNE
11-15 DECEMBER 1989

CONVECTION AND DISEQUILIBRIUM DURING THE SOLIDIFICATION OF A BINARY MELT

Ross C. KERR*, A.W. WOODS, M. G. WORSTER and H.E. HUPPERT

Dept. of Applied Mathematics and Theoretical Physics,
University of Cambridge, Silver Street, Cambridge CB3 9EW, ENGLAND

*Now at Research School of Earth Sciences, A.N.U.
G.P.O. Box 4, Canberra ACT, AUSTRALIA

ABSTRACT

The solidification of a binary melt cooled from above is investigated theoretically and experimentally. The partially solidified mushy layer is accurately modelled as a continuum whose growth is governed by the local interfacial supersaturation. Convection of the melt is shown to be important in determining both the rate of solidification and the development of compositional zonation in the final solid.

INTRODUCTION

When a melt of two or more components solidifies, the composition of the resulting solid is generally different from that of the melt. This compositional difference implies that the composition of the fluid in the near vicinity of the crystallization front differs from that in the bulk of the fluid and, consequently, that the density is also different. Differences in density can drive intense convective flows and thereby play a large role in solidifying systems.

Here we summarize recent investigations (Kerr *et al.*, 1989, 1990a,b,c) of cooling, from an upper horizontal boundary, a melt that releases less dense fluid on solidification. Several novel interactions between convection and solidification are introduced in turn and progressively incorporated into a mathematical model. Our theoretical predictions compare well with results from our laboratory experiments using aqueous solutions of isopropanol and sodium sulphate. These are easy to handle in the laboratory and mimic the behaviour of a wide variety of binary alloys with which it is much more difficult to conduct controlled experiments.

THE MODEL

The model system that forms the basis for our study is illustrated in figure 1. A rectangular container is filled with a binary melt of initially uniform composition C_0 and temperature T_0. At some time $t = 0$ the upper boundary is instantaneously cooled to, and subsequently maintained at, a temperature T_b that is lower than the liquidus temperature $T_L(C_0)$ of the solution. All the other boundaries are considered to be thermally insulated.

Our initial experiments used solutions of isopropanol and water, and a T_b greater than the eutectic temperature T_e. Ice formed at the upper boundary and grew downwards in thin plates to form the mushy layer depicted in figure 2. The fluid in the interstices of the mushy layer is enriched in isopropanol as a result of the selective growth of the ice. The enriched isopropanol solution is less dense than the original solution and remains stagnant within the mushy layer. Below the mushy layer we observed vigorous thermal convection of the fluid in response to the cooling from above. This convection plays an important role in the subsequent evolution of the system.

In order to evaluate the experimental results and to apply our findings to other systems, we have developed a mathematical model based on our understanding of the physical processes involved in the laboratory experiments. Equations governing heat and mass conservation within the mushy layer are derived from Worster (1986). Transport of heat is governed by thermal diffusion and is described by

$$c_m \frac{\partial T}{\partial t} = \frac{\partial}{\partial z}\left(k_m \frac{\partial T}{\partial z}\right) + \mathcal{L}_\beta \frac{\partial \phi}{\partial t}, \qquad (1)$$

where T is the local temperature and ϕ the local volume fraction of solid. Changes in ϕ result in an internal release of latent heat which must be conducted through the mushy layer. The thermodynamic parameters are the specific heat per unit volume c, the thermal

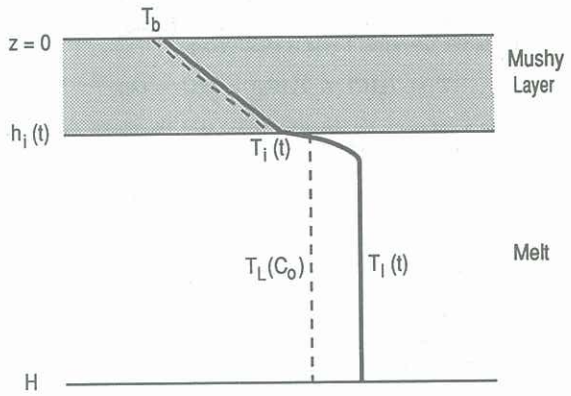

Fig. 1 Definition sketch for the growth of a mushy layer below a cold horizontal boundary maintained at a fixed temperature T_b. Throughout the mushy layer, the temperature (solid line) is equal to the liquidus temperature (dashed line) of the interstitial melt. The interfacial temperature T_i is less than the equilibrium freezing temperature of the melt $T_L(C_0)$. Vigorous convection of the melt keeps its temperature uniform. The boundary temperature is greater than the eutectic temperature T_e and a mushy layer forms adjacent to the cooled boundary.

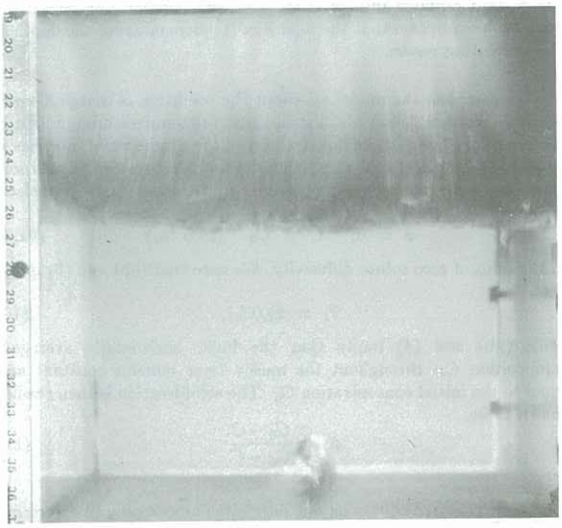

Fig. 2 A side view of the mushy layer in an isopropanol experiment. The mush consists of closely spaced, plate-like ice crystals and interstitial melt. This fine-scale structure allows the mushy layer to be treated theoretically as a continuum.

conductivity k and the latent heat per unit volume of solid $\mathcal{L}$. Subscripts 'β', 'm' and later 'l' denote properties of the solid phase, the mushy layer, and the liquid respectively. We evaluate the thermal properties of mushy layer by equating them to local averages, weighted by the volume fraction, of the properties of the constituent phases:

$$c_m = \phi c_\beta + (1 - \phi)c_l \tag{2}$$

and

$$k_m = \phi k_\beta + (1 - \phi)k_l. \tag{3}$$

Huppert & Worster (1985) and Worster (1986) demonstrate that the depth of a stagnant mushy layer is determined principally by thermal balances. Therefore, since the thermal diffusivity is typically much greater than the solutal diffusivity, we assume that vertical diffusion of solute is negligible. Conservation of solute in the mushy layer can then be expressed by

$$(1 - \phi)\frac{\partial C}{\partial t} = (C - C_\beta)\frac{\partial \phi}{\partial t}, \tag{4}$$

where C is the concentration of the interstitial liquid and C_β is the uniform concentration of the solid dendrites. Finally, we couple (1) and (4) via the linearized liquidus relationship

$$T = T_L(C) \equiv T_L(C_0) + \Gamma(C - C_0), \tag{5}$$

where Γ is a constant, on the assumption that the mushy layer is in local thermodynamic equilibrium.

Conservation of heat across the thermal boundary layer at the moving mush–liquid interface requires that

$$[c_l(T_l - T_i) + \mathcal{L}_\beta\phi]\,\dot{h}_i = k_m \left.\frac{\partial T}{\partial z}\right|_{z=h_i-} - F_T, \tag{6}$$

where $h_i(t)$ is the position of the interface, T_i is the temperature there and F_T is the convective heat flux from the liquid to the mushy region. Conservation of heat in the region of well-mixed liquid is expressed by

$$c_l(H - h_i)T_l = -F_T, \tag{7}$$

where H is the initial depth of the liquid. The heat flux F_T is approximated by the well known semi-empirical relationship for convective heat transfer

$$F_T = \lambda k_l \left(\frac{\alpha g}{\kappa_l \nu}\right)^{1/3} (T_l - T_i)^{4/3}, \tag{8}$$

where g is the acceleration due to gravity, α the coefficient of thermal expansion of the liquid, κ_l its thermal diffusivity, ν its kinematic viscosity and λ is an empirical constant. This relationship, which is often expressed in the dimensionless form $Nu \propto Ra^{1/3}$, where Nu is the Nusselt number and Ra is the Rayleigh number, can be derived from the assumption that the heat flux is independent of the depth of the convecting region.

To complete the model we adopt the condition of marginal equilibrium (Worster, 1986) which states that the temperature gradient in the boundary layer in the liquid ahead of the mush–liquid interface is equal to the gradient of the local liquidus temperature. This condition, combined with conservation of solute at the mush–liquid interface, leads to

$$\phi = 0, \quad C = C_0 \quad (z = h_i) \tag{9a,b}$$

in the limit of zero solute diffusivity. We note that (9b) and (5) imply that

$$T_i = T_L(C_0), \tag{10}$$

while (9b) and (4) imply that the bulk, horizontally averaged, composition C_H throughout the mushy layer remains constant and equal to the initial concentration C_0. The solid fraction is then readily shown to be

$$\phi = \frac{C_0 - C}{C_\beta - C} \tag{11}$$

This system of equations was integrated numerically to determine the evolution of h_i and T_l. Results are shown in figure 3 where they are compared with data from the experiments with isopropanol. Very good agreement is found between theory and experiment for the growth of the mushy layer (figure 3a) and the cooling rate of the solution (figure 3b). The data show that the temperature of the solution fell below the liquidus temperature during the course of each experiment. Such supersaturation, which cannot be accounted for with an equilibrium model, can have extremely important consequences for the evolution of the system, as we demonstrate below.

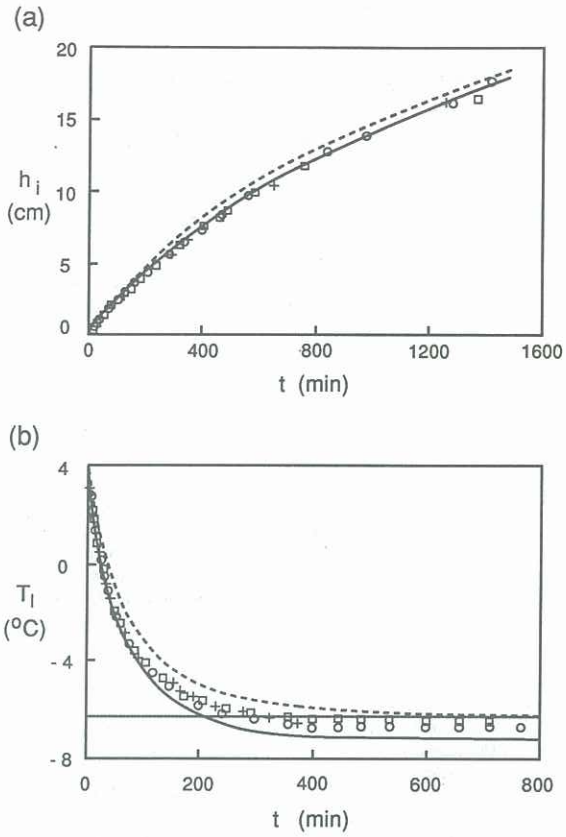

Fig. 3 (a) The depth of the mushy layer h_i and (b) the temperature of the solution T_l versus time including data obtained from isopropanol experiments in which $T_b = -25\,^\circ$C, $C_0 = 83.2$ wt.% H_2O, $T_0 = 4.0\,^\circ$C and $H = 18.8$cm. The dashed upper curve was calculated using the equilibrium assumption that the interface temperature T_i is equal to the initial liquidus temperature of the solution $T_L(C_0)$. The solid lower curve was calculated using the kinetic growth law (11) to determine T_i, and gives a better fit to the data. The horizontal dotted line in (b) indicates the liquidus temperature $T_L = -6.2\,^\circ$C. In the calculations $c_\beta = 1.832\,\mathrm{J\,cm^{-3}\,^\circ C^{-1}}$, $c_l = 3.912\,\mathrm{J\,cm^{-3}\,^\circ C^{-1}}$, $k_\beta = 0.022\,\mathrm{W\,cm^{-1}\,^\circ C^{-1}}$, $k_l = 0.0037\,\mathrm{W\,cm^{-1}\,^\circ C^{-1}}$, $\mathcal{L}_\beta = 306\,\mathrm{J\,cm^{-3}}$, $\nu = 0.057\,\mathrm{cm^2 s^{-1}}$, $\lambda = 0.056$ and the liquidus was represented by $T_L = -6.2 + 0.65(C - 83.2)$, where C is in wt.% H_2O and T_L is in $^\circ$C. All these values were determined from published data. Our own measurements suggested that $\alpha = (2.25 + 0.15\mathrm{T}) \times 10^{-4}\,^\circ\mathrm{C}^{-1}$, where T was taken to be the mean of T_i and T_l.

DISEQUILIBRIUM

Crystal growth is necessarily a non-equilibrium process; some supersaturation must exist in the vicinity of a growing crystal interface in order to drive solidification. Usually, the departures from equilibrium are small and good predictions of growth rates can be made by assuming that the system evolves through equilibrium states, as we have just seen. A more accurate model of crystal growth takes account of the interfacial kinetics involved by recognizing that the rate of growth is a function of the local supersaturation. We replace the equilibrium assumption leading to (10) by the simple linear relationship

$$\dot{h}_i = \mathcal{G}(T_L - T_i), \tag{12}$$

where T_L is the liquidus temperature at the interface and $\mathcal{G}$ is a constant. The interfacial temperature is now less than T_L and $C_i < C_0$. Correspondingly, since there is still no solute flux across the interface, the solid fraction at the interface, given by (11) with $C = C_i$, is greater than zero. By carefully measuring the evolution of the depth of the mushy layer $h_i(t)$ and the temperature at the interface T_i with a 1 mm bead thermistor during many experiments, we have confirmed (12) for the water–isopropanol system for supersaturations $T_L - T_i$ up to 3 °C and measured $\mathcal{G}$ to be approximately $2.2 \times 10^{-4}\,\mathrm{cm\,s^{-1}\,^\circ C^{-1}}$

The kinetic growth law (12) gives a timescale $\tau_{\mathcal{G}} = H/\mathcal{G}(T_L - T_b)$ associated with disequilibrium which can be compared with the timescale for thermal diffusion $\tau_k = H^2/\kappa$. The ratio $\epsilon = \tau_{\mathcal{G}}/\tau_k$ is typically very small; for example, it takes the value 1.2×10^{-2} for our experiments with isopropanol. This indicates that when diffusion is the only transport process (Huppert & Worster, 1985; Worster, 1986), departures from equilibrium are negligible except at times of order $\tau_{\mathcal{G}}$, which are very short compared with the solidification time, which is of order τ_k. However, we shall see that these small departures are important when coupled with convection of the melt.

The non-equilibrium model obtained by employing (13) rather than (9) gives excellent agreement with experimental data for the growth of the ice (see figure 3a). It also accounts for the occurrence of supersaturation in the liquid region after about 200 min. The discrepancy between the predicted and experimentally observed results for the level of supersaturation is due to heat gains from the laboratory.

SECONDARY CRYSTALLIZATION

The experiments with isopropanol solutions were meta-stable for much of their evolution. That is, had there been sites for nucleation within the supersaturated liquid region then crystals could have grown anywhere in that region in addition to the crystals growing within the mushy layer. Such secondary crystallization has been observed, both by us and by previous authors (Turner *et al.*, 1986), in laboratory experiments using various aqueous solutions. An example is shown in figure 4. In these cases the solid forming the dendrites in the mushy layer was denser than the solution, and nucleation sites for crystallization may have been provided by a few small crystals that settled from the mushy layer.

The crystallization at the floor locally depleted the melt of solute and produced a buoyant residual liquid, which caused compositional convection in the whole liquid region. The convection of solvent away from the growing crystals allowed for very efficient growth into the supersaturated liquid which we model by assuming that the crystals grew sufficiently rapidly to restore thermodynamic equilibrium to the liquid. This gives a strict upper bound on the rate of growth of the crystals on the floor and, as shown below, gives a good approximation for the observed growth. There is still kinetic undercooling at the mush–liquid interface as illustrated in the temperature profile of figure 5.

If the crystals on the floor are assumed to occupy a solid layer of thickness $h_f(t)$ then global conservation of solute demands that

$$\dot{h}_f = \frac{H - h_i - h_f}{C_\beta - C_l}\dot{C}_l, \tag{13}$$

where C_l is the time-dependent composition of the well-mixed liquid region. Our assumption that the secondary crystal growth restores equilibrium to the convecting liquid can be expressed by

$$T_l = T_L(C_l), \tag{14}$$

and the latent heat released modifies equation (7), which becomes

$$\mathcal{L}_\beta \dot{h}_f - c_l(H - h_i - h_f)\dot{T}_l - c_\beta h_f T_l = F_T. \tag{15}$$

While the release of solvent by the secondary crystal growth has an obvious direct effect on the liquid region, it also has an indirect effect on the evolution of the mushy layer. Even though there is no flux of solvent across the mush–liquid interface, the changing composition of the liquid implies that the composition of the solution incorporated into the advancing mushy layer decreases with time. Consequently, the bulk composition of the mushy layer is a function of height. In fact, since we have neglected vertical transport of solute within the mushy layer, the bulk, horizontally averaged, composition $C_H(z)$ is given simply by the composition of the liquid region at the time t_i when the position of the mush–liquid interface h_i was equal to z. That is

$$C_H(z) = C_l(t_i) \quad \text{where} \quad h_i(t_i) = z. \tag{16}$$

One effect of the variation in $C_H(z)$ is that the solid fraction within the mushy layer is altered

$$\phi = \frac{C_H(z) - C}{C_\beta - C}, \tag{17}$$

with consequent changes in the thermal properties (2) and (3) and the internal release of latent heat in (1). These changes all affect the rates of evolution of the system.

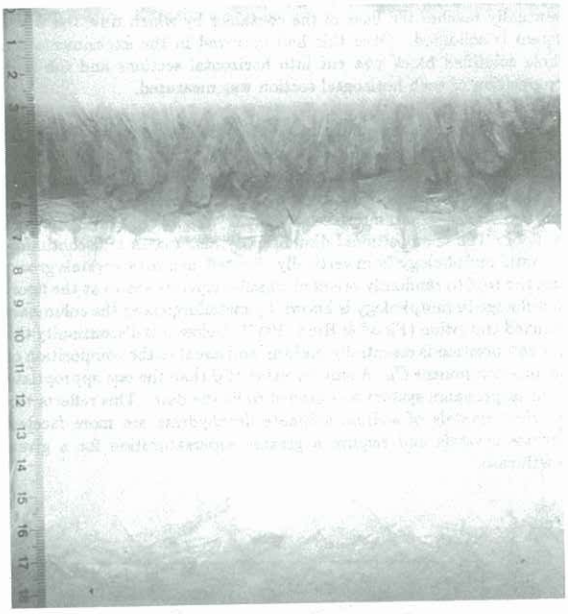

Fig. 4 A side view of an experiment in which an aqueous solution of Na_2SO_4 was cooled from above. It shows the growth of both a mushy layer and a layer of composite solid at the roof of the tank, and the growth of a layer of faceted $Na_2SO_4.10H_2O$ crystals at the base.

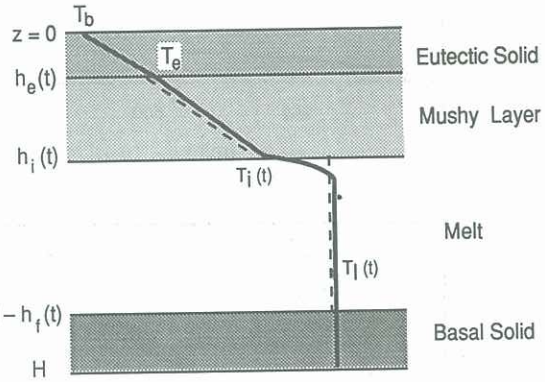

Fig. 5 Definition sketch, similar to figure 1, for the growth of a mushy layer below a cold horizontal boundary maintained at a fixed temperature T_b. There are two additional layers. The first is a layer of composite solid which grows on the roof when $T_b < T_e$. The second, which usually appears once the melt temperature T_l reaches $T_L(C_0)$, is a solid layer of crystals that grows on the base at a rate sufficient to keep the melt on the liquidus. The temperature within the basal solid is taken to be equal to T_l.

COMPOSITIONAL STRATIFICATION

A much more important consequence of the secondary solidification is that it provides an explanation of the compositional stratification that is often observed when binary melts are completely solidified. In order to investigate this effect quantitatively, we carried out experimental and theoretical investigations of systems in which the cooled upper boundary was maintained at a temperature T_b that was lower than the eutectic temperature T_e. A schematic diagram of such a system is shown in figure 5. A composite solid made up of crystals of the two pure end members of composition C_α and C_β occupies the region $0 \le z < h_e(t)$. Heat transfer across the layer is solely by conduction. At very early times T_i is less than T_e and there is no mushy layer. For most of the evolution, however, the temperature in this composite layer rises from T_b at $z = 0$ to T_e at $z = h_e$. Below the eutectic front $z = h_e$, the system looks much as before: a stagnant mushy layer extends from $z = h_e$ to $z = h_i$ and lies above a convecting liquid region. Secondary crystals growing near the base of the container fill a depth h_f from the floor. This structure can

be seen in the photograph in figure 4. The eutectic front $z = h_e$ eventually reaches the base of the container by which time the whole system is solidified. Once this had occurred in the experiments the whole solidified block was cut into horizontal sections and the bulk composition of each horizontal section was measured.

Results are shown in figure 6. We see, in figure 6b, that the mean composition decreases with depth from the top of the sample, which reflects the decreasing composition of the liquid region during the experiment. There is a jump in mean composition at the height where the mush–liquid interface met the crystal layer growing up from the floor. The compositional discontinuity also marks a discontinuity in crystal morphology from vertically oriented, dendritic crystals grown from the roof to randomly oriented, smaller crystals grown at the floor. This change in morphology is known by metallurgists as the columnar-equiaxed transition (Flood & Hunt, 1987). Below this discontinuity the bulk composition is essentially uniform and equal to the composition of the pure component C_β. A smaller value of $\mathcal{G}$ than the one appropriate to the isopropanol system was needed to fit the data. This reflects the fact that crystals of sodium sulphate decahydrate are more faceted than ice crystals and require a greater supersaturation for a given growth rate.

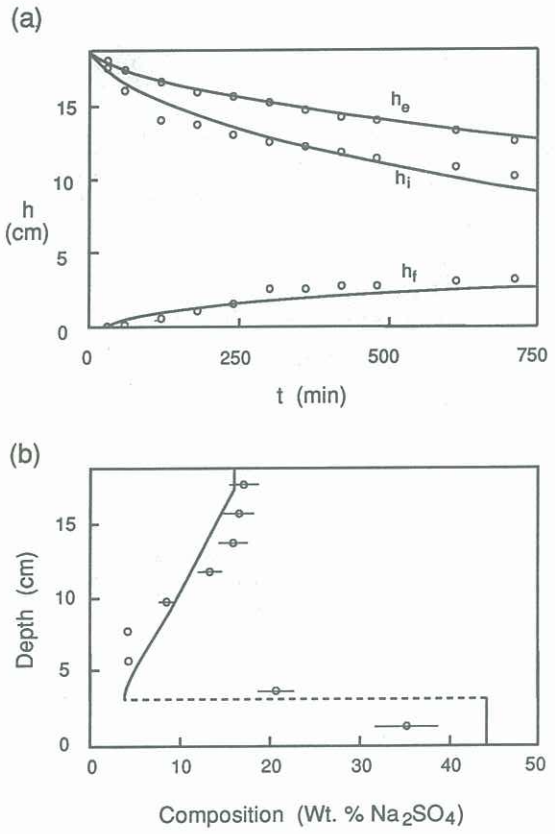

Fig. 6 (a) The thickness of the roof solid $h_e(t)$ (upper curve) and mushy layer $h_i(t)$ (central curve) measured from the top of the container (height 18.8 cm) and the basal solid $h_f(t)$ (lower curve) measured from the floor of the tank for the complete solidification of an aqueous solution of sodium sulphate. Circles are experimental data. (b) The compositional zonation of the final solid block as predicted by the theory and as measured in the experiment. The error bars indicate uncertainties due to the melting of the solid while it is being cut into the 2 cm thick horizontal sections for sampling. This has been indicated by the error bars. In the calculations $c_l = 4.1\,\mathrm{J\,cm^{-3}{}^\circ C^{-1}}$, $c_\beta = 2.66\,\mathrm{J\,cm^{-3}{}^\circ C^{-1}}$, $\mathcal{L}_\beta = 337\,\mathrm{J\,cm^{-3}}$, $\mathcal{L}_\alpha = 306\,\mathrm{J\,cm^{-3}}$, $\nu = 0.023\,\mathrm{cm^2 s^{-1}}$, $k_l = 0.0059\,\mathrm{W\,cm^{-1}{}^\circ C^{-1}}$, $k_\beta = 0.008\,\mathrm{W\,cm^{-1}{}^\circ C^{-1}}$, $k_\alpha = 0.022\,\mathrm{W\,cm^{-1}{}^\circ C^{-1}}$, $\lambda = 0.056$, $\alpha = (0.2 + 0.24T_l) \times 10^{-4}\,{}^\circ\mathrm{C}^{-1}$ where T_l is the liquidus temperature of the melt. The initial melt temperature and composition were 30.5 °C and 16 wt.% Na_2SO_4. The liquidus curve was calculated with a cubic spline using published data. The kinetic growth parameter used was $\mathcal{G} = 1.5 \times 10^{-4}\,\mathrm{cm\,s^{-1}{}^\circ C^{-1}}$

DISCUSSION

At a fundamental level, the agreement between the results of our theoretical model and experiments validates our description of the mushy layer and its simulation as a continuum. There are many practical applications of this macroscopic approach to various situations considered by crystal growers and metallurgists. There are also important geological applications, for example to the understanding of the cooling and solidification of lava flows and magma chambers. Equilibrium models of solidification will accurately predict the removal of any superheat from the lava and the initial formation of a dendritic crust but, in such models, the interior of the lava cannot cool below its initial liquidus temperature. In contrast, the present models show that the coupling of fluid-mechanical and disequilibrium effects can cause additional crystallization of the lava, either at the base of the flow or in its interior. This secondary solidification changes the composition of the lava, which lowers the liquidus temperature and allows cooling and convection to continue. Our study demonstrates further how the changing composition of the melt results in a stratification of the bulk composition of the mushy layer. It also provides a mechanism for the redistribution of solute during the complete solidification of an alloy cooled from above. Such macrosegregation is observed in completely solidified ingots and in igneous rocks.

ACKNOWLEDGEMENTS

We wish to thank Mark Hallworth for his invaluable technical assistance with the experiments. J. Dantzig, A. Hoadley, D. Hurle, C. Jaupart, J. Lister and J.S. Turner provided many valuable comments. We gratefully acknowledge research fellowships from the following Cambridge Colleges: Churchill (R.C.K.), Trinity (M.G.W.) and St. John's (A.W.W.); and also the financial support of the B.P. Venture Research Unit (H.E.H.).

REFERENCES

FLOOD, S.C. & HUNT, J.D. (1987) A model of a casting. *Appl. Sci. Res.* 44, 27–42.

HUPPERT, H.E. & WORSTER, M.G. (1985) Dynamic solidification of a binary alloy. *Nature* 314, 703–707.

KERR, R.C., WOODS, A.W., WORSTER, M.G. & HUPPERT, H.E. (1989) Disequilibrium and macrosegregation during solidification of a binary melt. *Nature* 340, 357–362.

KERR, R.C., WOODS, A.W. WORSTER, M.G. & HUPPERT, H.E. (1990 a,b,c) Solidification of an alloy cooled from above. Part I: Equilibrium growth. Part II: Nonequilibrium interfacial kinetics. Part III: Compositional stratification within the solid. *J. Fluid Mech.*, submitted.

TURNER, J.S., HUPPERT, H.E. & SPARKS, R.S.J. (1986) Komatiites II: Experimental and theoretical investigations of post-enplacement cooling and crystallization. *J. Petrol.* 27, 397–437.

WORSTER, M.G. (1986) Solidification of an alloy from a cooled boundary. *J. Fluid Mech.* 167, 481–501.